Echocardiography

Petros Nihoyannopoulos • Joseph Kisslo Editors

Echocardiography



Editors
Petros Nihoyannopoulos, MD, FRCP
Imperial College London
National Heart and Lung Institute
Hammersmith Hospital
London
UK

Joseph Kisslo, MD Division of Cardiovascular Medicine Duke University Medical Center Durham, NC USA

ISBN 978-1-84882-292-4 e-ISBN 978-1-84882-293-1 DOI 10.1007/978-1-84882-293-1 Springer Dordrecht Heidelberg London New York

British Library Cataloguing in Publication Data A catalogue record for this book is available from the British Library

Library of Congress Control Number: 2009927906

© Springer-Verlag London Limited 2009

Apart from any fair dealing for the purposes of research or private study, or criticism or review, as permitted under the Copyright, Designs and Patents Act 1988, this publication may only be reproduced, stored or transmitted, in any form or by any means, with the prior permission in writing of the publishers, or in the case of reprographic reproduction in accordance with the terms of licenses issued by the Copyright Licensing Agency. Enquiries concerning reproduction outside those terms should be sent to the publishers.

The use of registered names, trademarks, etc., in this publication does not imply, even in the absence of a specific statement, that such names are exempt from the relevant laws and regulations and therefore free for general use.

Product liability: The publisher can give no guarantee for information about drug dosage and application thereof contained in this book. In every individual case the respective user must check its accuracy by consulting other pharmaceutical literature.

Printed on acid-free paper

Springer is part of Springer Science+Business Media (www.springer.com)

Preface

Echocardiography has expanded greatly over recent years to earn its place as a subspecialty in cardiology in its own right. From the original single M-mode modality of 50 years ago, it has evolved into a complex "multimodality" method for evaluating and quantifying cardiovascular lesions. In addition, the entire spectrum of hemodynamic assessment of the heart can now be performed noninvasively using echocardiography alone. Transesophageal echocardiography has added to the clarity of imaging and proved to be extremely helpful in valve surgery. Lately, three-dimensional echocardiography has added a new dimension and helped the understanding of cardiac anatomy and pathology in real time. Finally, deformation imaging and assessment of myocardial perfusion complete the global assessment of the heart by echocardiography by looking at the various contraction and perfusion patterns in patients with coronary artery disease at rest and during stress.

Echocardiography highlights the clinical utility of these evolving modalities that are now crucial to the renaissance of echocardiography. This book provides a thorough clinical review of the most revealing and adaptable echocardiographic methods of imaging a patient. The editors and their world-class group of contributors have created an essential reference for all who use echocardiography in the practice.

London, UK Durham, NC Petros Nihoyannopoulos Joseph Kisslo

Contents

Section 1 How Things Work

1	Physical Principles and the Basic Exam	3		
2	Conducting a Cardiac Ultrasound Examination	31		
3	Principles of Flow Assessment	47		
4	Principles of Hemodynamic Assessment	63		
5	Tissue Doppler, Doppler Strain, and Non-Doppler Strain: Tips, Limitations, and Applications Diala Khraiche and Denis Pellerin	79		
6	Transesophageal Echocardiography: Principles and Application Partho P. Sengupta and Bijoy K. Khandheria	101		
Section 2 Valvular Heart Disease				
7	Aortic Valve Disease: A. Aortic Stenosis Petros Nihoyannopoulos	117		
8	Mitral Valve Disease	135		
9	Tricuspid and Pulmonic Valve Disease	215		
10	Pulmonary Hypertension Clinical Echocardiography	229		

viii Contents

11	Criteria for Operative Intervention in Valvular Heart Disease Based on Echocardiography	251		
	William J. Stewart	231		
12	Clinical Echocardiography Prosthetic Valves	265		
13	The Use of Echocardiography in the Diagnosis and Treatment of Patients with Infective Endocarditis	283		
Sec	tion 3 Pericardial Disease			
14	Pericardial Effusion, Tamponade, and Constriction Teresa S.M. Tsang, Larry J. Sinak, and Jae K. Oh	297		
Sec	tion 4 Ventricular Disorders and Ischemic Disease			
15	Clinical Echocardiography: Coronary Artery Disease: Assessing Regional Wall Motion Paramjit Jeetley and Roxy Senior	313		
16	Stress Echocardiography Thomas Marwick	325		
17	Principles of Myocardial Viability Implications for Echocardiography Jean-Louis J. Vanoverschelde, Agnès Pasquet, Bernhard Gerber, and Jacques A. Melin	351		
18	Echocardiography for Assessing Acute Myocardial Infarction Otto Kamp and Cees A. Visser	367		
19	Mechanical Complications of Myocardial Infarction Daniel Monakier and Harry Rakowski	385		
20	Cardiomyopathies	399		
21	Echocardiography in Heart Failure	435		
22	Cardiac Resynchronization Therapy	447		
Section 5 Masses, Emboli and Trauma				
23	Intracardiac Masses William Smith, David Adams, and Joseph Kisslo	465		

Contents

24	Aortic Disorders	473		
	Ayan R. Patel, Stefano De Castro, and Natesa G. Pandian			
25	Source of Embolus	489		
	Patrick J. Nash, Ronan J. Curtin, and Allan L. Klein			
Section 6 Congenital Heart Disease				
26	Simple Congenital Heart Defects	513		
	George A. Pantely and Michael A. Gatzoulis			
27	Echocardiographic Evaluation of Complex Congenital Heart Disease	525		
	Marcy L. Schwartz and Gerald R. Marx			
28	Adult Congenital Heart Disease	541		
Sec	tion 7 Special Methods			
29	Intraoperative Echocardiography	569		
30	Contrast Echocardiography Mark J. Monaghan	581		
31	Three-Dimensional Echocardiography	603		
32	Ultrasound Stethoscopy Eleni C. Vourvouri, and Jos R.T.C. Roelandt	619		
33	Echo-Guided Interventions	637		
Ind	ex	655		

Contributors

David B. Adams, RCS, RDCS

Department of Cardiology, Echo Lab, Duke University Medical Center, Durham, NC, USA

Ahmed A. Alsaileek, MD

Department of Cardiac Science, King Abdulaziz Medical City, Riyadh, Kingdom of Saudi Arabia

Christopher H. Cabell, MD, MHS

Duke University Medical Center, Durham, NC, USA

John B. Chambers, MD, FRCP, FESC, FACC

Cardiothoracic Centre, St. Thomas Hospital, London, UK

Ronan Curtin, MB, BCh, BAO, MSc, MRCPI

Department of Cardiovascular Medicine, The Cleveland Clinic, Cleveland, OH, USA

Stefano De Castro

Department of Cardiovascular, Respiratory and Morphological Sciences, University of Rome Rome, Italy

Meeney Dhir, MD, FACC, FASE

Sonterra Cardiovascular Institute PA, San Antonio, TX, USA

Kate M. English, MB, ChB, MRCP, PhD

Yorkshire Heart Centre, Leeds General Infirmary, Leeds, UK

Emily Forsberg, BSRT, RDCS-AE, PE

Department of Non-Invasive Cardiology, Park Nicollet Methodist Hospital, St. Louis Park, MN, USA

Michael A. Gatzoulis, MD, PhD, FACC, FESC

Department for Pulmonary Hypertension, Royal Brompton Hospital and the National Heart & Lung Institute, Imperial College, London, UK

Bernhard Gerber, MD, PhD, FESC

Division of Cardiology, Université Catholique de Louvain, Brussels, Belgium

J. Simon R. Gibbs, MA, MD, MB, BChir, FRCP

National Heart and Lung Institute, Imperial College, London, UK

John L. Gibbs, FRCP

Yorkshire Heart Centre, Leeds General Infirmary, Leeds, UK

xii Contributors

Donald D. Glower, MD

Duke University Medical Center, Durham, NC, USA

Paramjit Jeetley, MBChB, MRCP (UK)

Department of cardiology, Bristol Royal Infirmary, Bristol, Avon, UK

James J. Jollis, MD

Duke University Medical Center, Durham, NC, USA

Otto Kamp, MD, PhD

Department of Cardiology, VU University Medical Center, Amsterdam, The Netherlands

Bijoy K. Khandheria, MBBS, MD, FACC, FESC, FASE

Cardiovascular Division, Mayo Clinic Arizona, Scottsdale, AZ, USA

Diala Khraiche

The Heart Hospital, London, UK

Joseph Kisslo, MD

Division of Cardiovascular Medicine, Duke University Medical Center, Durham, NC, USA

Allan L. Klein, MD, FRCP, FACC, FAHA, FASE

Department of Cardiovascular Medicine, The Cleveland Clinic, Cleveland, OH, USA

Graham J. Leech, MA

Department of Cardiovascular Science, St. George's Hospital Medical School, London, UK

Wei Li, MD, PhD

Department of Echocardiography and Adult Congenital Heart Disease, Royal Brompton and Harefield NHS Trust, London, UK

Burkhard G. Mackenson, MD

Duke University Medical Center, Durham, NC, USA

Thomas Marwick, MBBS, PhD

University of Queensland, School of Medicine, Princess Alexandra Hospital, Brisbane, QLD, Australia

Gerald R. Marx, MD

Department of Cardiology, Boston Children's Hospital, Boston, MA, USA

Jacques A. Melin, MD, PhD

Division of Cardiology, Université Catholique de Louvain, Brussels, Belgium

Mark J. Monaghan, MSc, PhD

Department of Cardiology, King's College Hospital, London, UK

Daniel Monakier, MD

Toronto General Hospital, Toronto, ON, Canada

Patrick J. Nash, MD, BCh, BAO, FRCPI

Department of Cardiology, Galway University Hospital, Galway, Ireland

Petros Nihoyannopoulos, MD, FRCP, FACC, FESC

Imperial College London, National Heart and Lung Institute,

Hammersmith Hospital, London, UK

Contributors xiii

Jae K. Oh, MD

Department of Cardiology, Mayo Clinic, Rochester, MN, USA

Natesa G. Pandian, MD

Division of Cardiology, Tufts-New England Medical Center, Boston, MA, USA

George A. Pantely, MD

Department of Cardiovascular Medicine, Oregon Health & Science University, Portland, OR, USA

Agnès Pasquet, MD, PhD

Division of Cardiology, Université Catholique de Louvain, Brussels, Belgium

Ayan R. Patel, MD

Division of Cardiology, Tufts-New England Medical Center, Boston, MA, USA

Denis E. Pellerin, MD, PhD

The Heart Hospital, London, UK

Harry Rakowski, MD, FRCPC, FACC, FASE

Toronto General Hospital, Toronto, ON, Canada

J. Daniel Rivera, CVT

Duke University Medical Center, Durham, NC, USA

J.R.T.C. Roelandt, MD, PhD

Department of Cardiology, Erasmus MC, Rotterdam, The Netherlands

Robert M. Savage, MD, FACC

Departments of Cardiothoracic Anesthesia, and Cardiovascular Medicine, The Cleveland Clinic Foundation, Cleveland, OH, USA

Marcy L. Schwartz, MD

Department of Cardiology, Cleveland Clinic, Cleveland, OH, USA

Partho P. Sengupta, MBBS, MD, DM

Cardiovascular Division, Mayo Clinic Arizona, Scottsdale, AZ, USA

Roxy Senior, MD, DM, FRCP, FESC, FACC

Department of Cardiology, Northwick Park Hospital, Harrow, Middlesex, UK

Frank E. Silvestry, MD, FASE

Cardiovascular Division, Department of Medicine, Radnor, PA, USA

Larry J. Sinak, MD

Department of Cardiology, Mayo Clinic, Rochester, MN, USA

William Smith, MD

Division of Cardiovascular Medicine, Duke University Medical Center, Durham, NC, USA

Alexander Stefanidis, MD, FACC, FASE

Section of Cardiovascular Imaging, Department of Cardiovascular Medicine, General Hospital of Nikaias, Piraeus, Greece

William J. Stewart, MD

Department of Cardiovascular Disease, The Cleveland Clinic, Cleveland, OH, USA

xiv Contributors

Jamil A. Tajik, MD, FACC

Mayo Graduate School of Medicine, Mayo Clinic, Rochester, MN, USA

Teresa S.M. Tsang, MD

Division of Cardiovascular Diseases, Department of Medicine, Mayo Clinic, Rochester, MN, USA

Jean-Louis J. Vanoverschelde, MD, PhD

Department of Cardiology, Cliniques Universitaires St-Luc, Brussels, Belgium

Cees A. Visser*, MD, PhD

Department of Cardiology, VU University Medical Center, Amsterdam, The Netherlands

Eleni C. Vourvouri, MD, PhD, FESC

Thoraxcentre, Erasmus MC, Rotterdam, The Netherlands

William A. Zoghbi, MD

Department of Cardiology, The Methodist DeBakey Heart Center, The Methodist Hospital, Houston, TX, USA

Section 1 How Things Work

Chapter 1 Physical Principles and the Basic Exam

Graham Leech

Introduction

The modern cardiac ultrasound scanner is a very sophisticated piece of equipment. It provides the ability to generate moving images of the heart, together with quantitative data on blood flow and tissue motion. The output is displayed in real time, either as two-dimensional (2-D) tomographic ("slice") images or, more recently, rendered three-dimensional (3-D) "volume" images from which individual sectional planes can be extracted. Although much of the pioneering development in echocardiography was carried out by researchers in academic institutions and small, innovative companies, the cost of developing, manufacturing and supporting the products is now such that the machines are now produced by almost exclusively by multinational electronics corporations.

Most of us drive a car without understanding the intricacies of an automatic gearbox or fuel injection, and we use computers without any need to know how the digital data within them are routed, and computations made millions of times each second. Furthermore, much of the information on the construction of ultrasound transducers and the image processing algorithms employed in the scan converters are closely guarded commercial secrets. Nevertheless, almost every textbook and training course in echocardiography (this volume being no exception) begins with a discussion on "Physics." The positive view is that some knowledge of the principles of ultrasound imaging is fundamental to understanding clinical applications, but there is no doubt that many students regard it as a "necessary

G. Leech
Department of Cardiovascular Science,
St. George's Hospital Medical School, London, UK
e-mail: graham@cardiac.demon.co.uk

evil," to be endured and then forgotten once they have moved on to the clinical applications. Conscious of these facts, the aim of this chapter will be restricted to three areas:

- (a) Basic understanding of how images and flow velocity data are obtained
- (b) The major user control functions in the machines and how they affect image quality
- (c) How limitations both of fundamental physics and current technology can result in image distortion and artifact that not infrequently result in serious misdiagnoses

Basic Concepts

Echocardiography employs high-frequency sound (pressure) waves to generate images of the heart and to study blood flow within the cardiac chambers and blood vessels. It is closely analogous to radar and the reader familiar with the way in which information from radar or a marine depth-sounder is gathered and displayed will recognize many similarities in the two techniques. Because there are fundamental differences in the physical principles underlying imaging of the heart's structure and studying blood flow, these will be considered separately, whereas in practice images and blood flow data are usually displayed and recorded superimposed or concurrently.

Pressure waves are generated by a vibrating object, and are transmitted through a solid, liquid, or gaseous medium as pressure fluctuations – waves of alternating compression and rarefaction. The velocity at which a medium propagates waves is primarily determined by its density, being higher in a solid, whose molecules are close together, than in a liquid or a gas.

Pressure waves travel in air at approximately 300 m.s⁻¹, and in soft body tissues the average value is about 1,540 m.s⁻¹. There is a fundamental relationship between propagation velocity, the frequency (pitch) of the waves and their wavelength (the distance between two successive maxima or minima in the train of pressure cycles).

This states that:

propagation velocity = frequency \times wavelength

Thus, in soft body tissues, at a frequency of 1,000 Hz (=Hertz or cycles per second), the wavelength is 1.54 m. Commonsense dictates that this is too great to image the heart, which is only about 15 cm across and which contains structures less than 1 mm thick. To achieve a wavelength of 1 mm, the frequency has to be 1,540,000 Hz or 1.54 MHz. Such high frequencies cannot be detected by the human ear, which responds only to frequencies from about 30 to 15,000 Hz, and since the word "sound" implies a sensation generated in the brain, the term, "Ultrasound" is used to describe them.

Pressure waves and light waves share many properties. When a beam of light passes from one medium to another, part of the energy is reflected and the path of the transmitted portion is deviated by refraction. In the same way, when pressure waves encounter an interface between two different body tissues, blood and muscle for example, some of the incident energy is reflected. Another characteristic shared by light and pressure waves is diffraction, whereby the waves "bend" around the edge of an obstacle. The degree to which this is apparent depends on the relative sizes of the wavelength and the obstacle. Thus sound waves, whose wavelength in air is of the order of 1 m, appear to bend around a given obstacle much more than light waves, having a wavelength of 0.000001 m. Ultrasound used for medical imaging typically has a wavelength of the order of 0.001 m (1 mm), half-way between that of sound and light. Ultrasound can therefore be thought of as being similar to a rather poorly focused flashlight; it can be formed into a beam and aimed at regions of the heart of interest, but is far from an infinitely fine "laser" probe. The ultrasound beam comprises a central main beam, which diverges with increasing distance from the transducer, surrounded by a number of smaller, secondary beams called "side lobes." These arise from the physics of wave propagation, and from the fact that the ultrasound transducer comprises a number of individual crystal elements.

Ultrasound waves are usually generated and detected by ceramic crystals, which exhibit strong piezoelectric properties. This means that they change their shape when an electric potential is applied to them and, conversely, they generate an electric charge when mechanically deformed. Because they convert electric energy into mechanical, and vice versa, they are called transducers. The material that has been used almost exclusively for imaging transducers is Lead Zirconate Titanate. This normally is in the form of a polycrystalline ceramic material and is "polarized" by applying an electric field to align the electrical axes of the microscopic crystals. The alignment is, however, not perfect but a new process has been introduced recently, which allows production of large, single crystals, which have a single polarization axis, and this promises to improve transducer performance significantly. An echocardiographic transducer comprises one or more such crystals, mounted on an absorbent backing. When electric impulses are applied to the crystal, it vibrates at a frequency determined by its mechanical dimensions, in the same way that a bell vibrates when struck by a hammer. Transducers used for echocardiography typically generate frequencies in the range 1.5–7 MHz. The same crystal is used to detect returning echoes from ultrasonic waves it has generated.

Imaging of Cardiac Structures

The Ultrasound Beam

Images of cardiac structures are formed by transmitting a stream of very brief "pulses" of ultrasonic waves into the thorax. Each pulse comprises only a few waves and lasts 1-2 microseconds (ms). As a pulse travels through the chest wall, the pericardium, and the heart, it crosses a succession of interfaces between different types of tissue: blood, muscle, fat, etc. At each interface, a proportion of the incident energy is reflected, the remainder being transmitted into deeper tissue layers. Provided that the interfaces are extensive compared to the ultrasound wavelength, the reflections are specular (mirror-like) with the angle of reflection equal to the angle of incidence with respect to a normal to the interface. Only if the incident angle is 90° will the reflected waves re-trace the incident path and return to the transducer as an echo.

This is not always easy to achieve in practice and limits the quality of echo signals from many cardiac structures, though the fact that body tissue interfaces are not totally smooth allows return of some echoes even if the interface is not perpendicular to the ultrasound beam. The transmitted portion of the ultrasound pulse may then encounter additional interfaces and further echoes return to the transducer.

The time delay between transmission of an ultrasound pulse and arrival of an echo back at the transducer (round-trip-time) is given by

Time delay = $2 \times \text{interface distance/propagation}$ velocity

Thus, if the propagation velocity is known and the time delay can be measured, the distance of each echogenerating interface from the transducer can be determined. It is important to note that the machine actually measures *time delay* and derives the *distance* from an assumed value for the propagation velocity in soft tissues. If, however, the ultrasound passes through an object having different transmission characteristics from soft tissue, e.g., a silicone ball valve prosthesis, the time delay of returning echoes will change and the derived distance measurements will be false.

The total time for all echoes to return depends on the distance of the furthest structure of interest. This may be up to 24 cm, for which the round trip time in soft tissue is approximately 300 ms. Only then can a second ultrasound pulse be transmitted, but even so it is possible to send more than 3,000 pulses each second. This stream of brief ultrasound pulses emanating from the transducer is referred to as an "ultrasound beam." The first echoes to return and strike the piezoelectric crystal arise from structures closest to the transducer, followed in succession by those from more distant interfaces. The minute electrical signals thus generated are amplified and processed to form a visual display showing the relative distances of the reflecting structures from the transducer, with the signal intensities providing some information about the nature of the interfaces.

The 2-D Sector Image

In order to generate 2-D tomographic (slice) images of the heart, the ultrasound beam has to be scanned across a section of the heart. The limited access to the heart afforded by spaces between the ribs and lungs dictates that cardiac scanners are of the sector scan type. The transducer is positioned on the chest manually and held steady, but the ultrasound beam it generates sweeps rapidly to and fro across a sector of an arc, creating a fan-shaped scan in the same way that a lighthouse beam sweeps across the sea, illuminating objects in its path. In order to avoid blurring of the image by the heart's motion, at least 25 images per second are required. The maximum attainable image frame rate is primarily the result of a trade-off between the required image depth, which limits the number of pulses transmitted per second, and the sector angle and image line density, but other factors such as the display mode and imaging processing power of the machine are now involved. Image frame rate shown on the display screen may be as high as 150 s⁻¹ or as low as 6 s⁻¹. It can be improved by reducing image depth and/or narrowing the scan angle.

Almost all commercial echo machines use "phased array" technology to scan the ultrasound beam. Using sophisticated equipment derived from that used to cut silicon for manufacturing electronic "chips," a single piezoelectric crystal is sliced into as many as 256 very thin strips, each connected individually to the electric pulse generator, which activates them in a very rapid and very precisely controlled sequence, as shown in Fig. 1.1. The wavelets from each crystal element merge to form a compound ultrasound wave. By varying the electrical activation sequence, the direction of the compound wave can be changed and a series of pulses generated to form a sector scan configuration. For a sector angle of 90° and working depth of 15 cm, each image comprises about 200 scan lines and takes about 40 ms.

Immediately after each pulse is transmitted, echoes start to return. The minute electrical signals they generate as they strike the transducer and deform its crystal elements are first amplified, then demodulated, which removes the ultrasound-frequency waves leaving just their envelope. The echo signals resulting from a single ultrasound pulse now comprise a sequence of electronic "blips" representing the intensities of the echo reflections it generated (Fig. 1.2). To facilitate further processing these are "digitized" – converted into a series of numbers, whose values represent the echo amplitudes at discrete intervals – and allocated to a digital memory store.

The basic image data comprise a series of radial scan lines like spokes of a wheel which are relatively

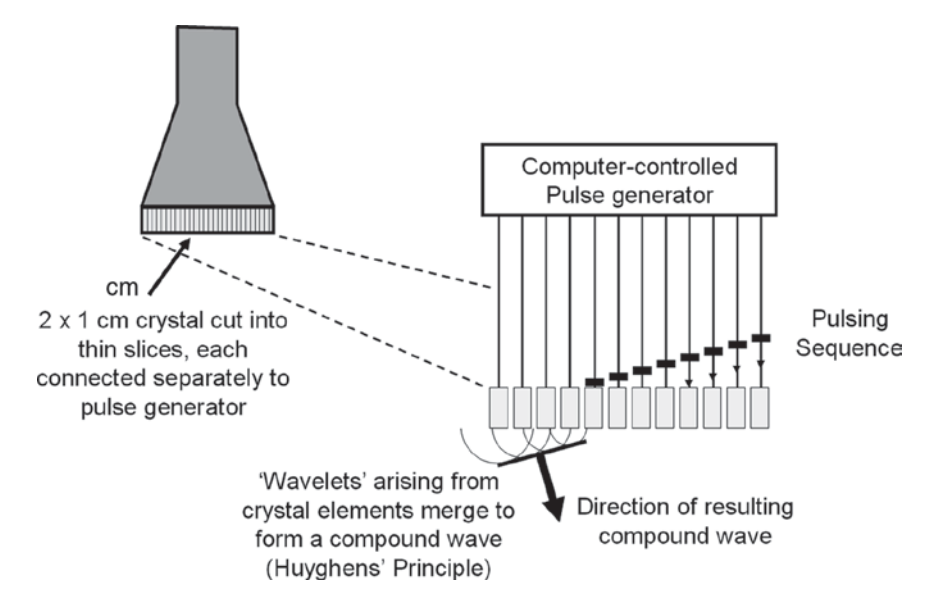


Fig. 1.1 How the ultrasound beam direction is controlled by pulsing the crystal elements in sequence

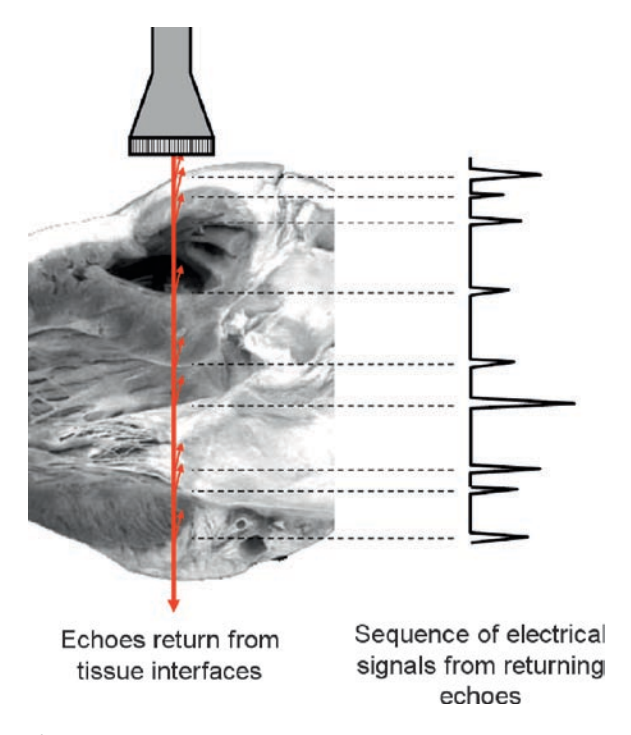


Fig. 1.2 Echoes returning from tissue interfaces are converted into electrical impulses

close together near to the transducer, but deeper into the thorax there are significant gaps between them (Fig. 1.3). In the earliest 2-D scanners of the 1970s, this line structure was evident (Fig. 1.4), but nowadays it is masked by assigning image values to the "empty" memory cells based on averages of surrounding cells. The averaging process employs proprietary algorithms which account in large part for the differences in image texture that are characteristic of the various brands of machine. From this stage onward, the image is represented by a matrix of numbers, enabling the power of the digital computer to be harnessed to process them further and form the visual display on the monitor screen.

M-Mode

In the earliest echo machines, the ultrasound beam was fixed, with the only steering provided by the operator's hand. The beam thus only interrogated structures along a single axis, a so-called "ice-pick" or "needle biopsy" view, with tissue interfaces represented as dots on the display screen. In order to show motion patterns, a linear sweep is added resulting in a graphic display as shown in Fig. 1.5. Though harder for the non-specialist to understand and considered by some to be "old fashioned," the M-mode display still offers important benefits: it shows data from several cardiac cycles on a single image; it provides temporal continuity making it easier, for example, to identify a structure such as the endocardium from background clutter; and it has far greater temporal resolution (1,000 lines.s⁻¹ compared to 25 for a 2-D image), making it superior for accurate

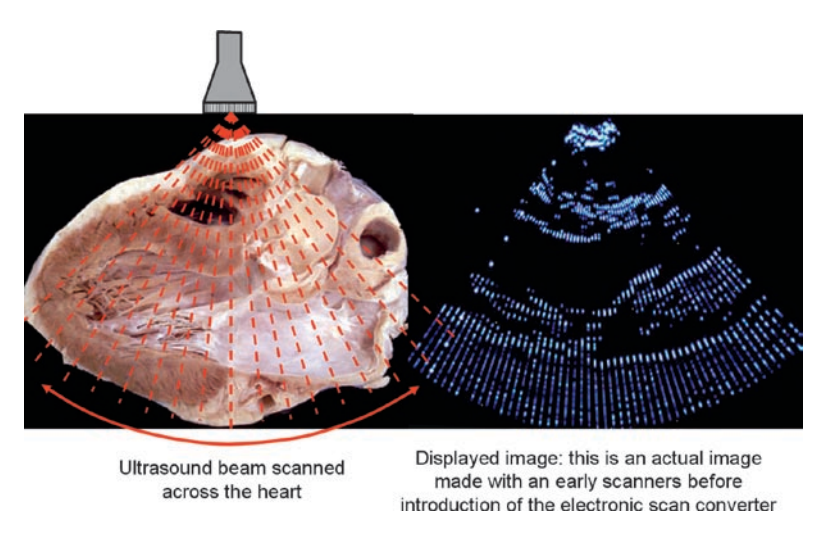


Fig. 1.3 The ultrasound beam is scanned rapidly to and fro across the heart and the echo signals are converted into an electronically generated image

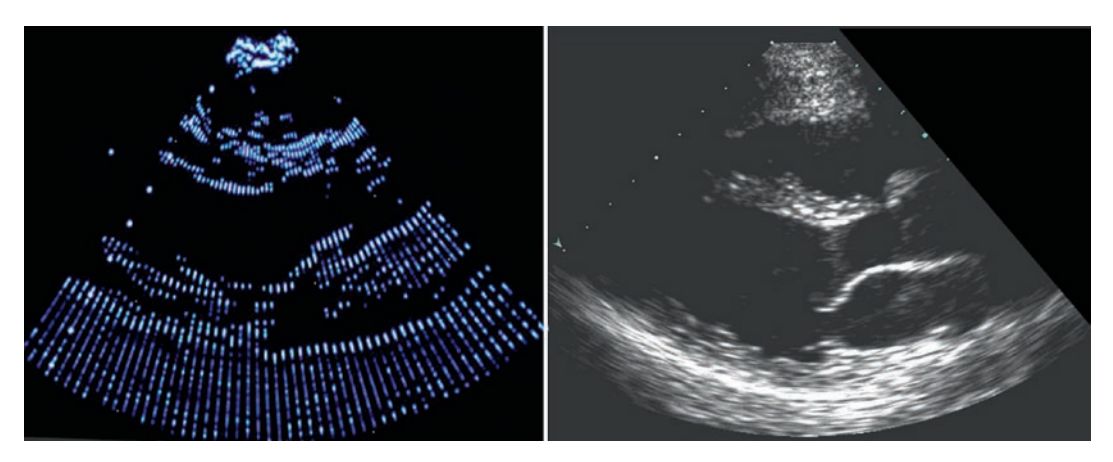


Fig. 1.4 (*Left*) Ultrasound image made in 1977 prior to introduction of scan converters and (*right*) from a modern machine. The scan converter interpolates the spaces between the actual scan lines and creates a more esthetically pleasing image, but does not add new information

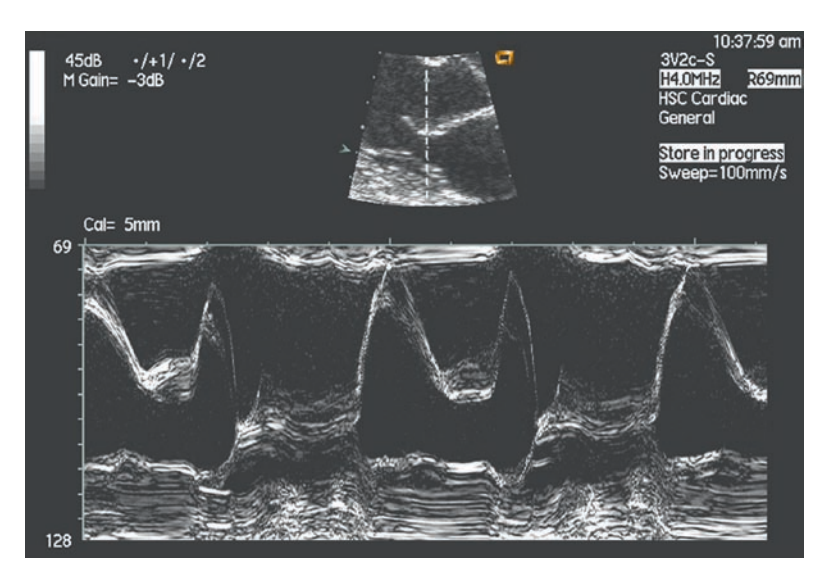


Fig. 1.5 "M-mode" display of the motion pattern of the mitral valve. The beam direction is indicated on the small image icon at the top of the display

timing and resolution of rapid movements such as a vibrating valve prosthesis.

Attenuation, Reflection and Depth Compensation

Attenuation: Ultrasound can travel great distances in water, but soft body tissues are "spongy" and nonhomogeneous, resulting in attenuation of the ultrasound waves. The degree of attenuation depends greatly on the frequency. At 2.5 MHz, approximately half of the amplitude is lost for every 4 cm of path length, rising to half per 2 cm at 5 MHz and half in only 1 cm at 7.5 MHz. This is a cumulative effect, so at 5 MHz the wave amplitude reaching a structure 16-cm distant is only 1/256 ($\frac{1}{2} \times \frac{1}{2} \times \frac{1}{2}$) of that transmitted.

Reflection: The proportion reflected at a tissue interface depends mainly on the difference in density of the tissues. Where there is a large difference, such as an interface with air or bone, most of the incident energy is reflected, creating an intense echo but leaving little to penetrate further to deeper structures. It is for this reason that the operator has to manipulate the transducer to avoid ribs and lungs, and that a contact gel is used to eliminate any air between the transducer and the chest wall. In contrast, there is relatively little difference in the densities of blood, muscle and fat, so echoes from interfaces between them are very small something like 0.1% of the incident amplitude. The echoes are then further attenuated as they return to the transducer, with the result that the amount reaching the transducer is very small indeed. In the case illustrated, approximately $(1/256) \times (1/1,000) \times (1/256)$ or just 1/65,000,000 of the transmitted amplitude!

Depth compensation: Not only is this a very small signal to detect, but the amplification level required would be vastly greater than that needed for the same interface at a range of 4 cm, for which the returning signal would be approximately $(1/4) \times (1/1,000) \times (1/4)$ or 1/16,000. To overcome this problem, the machine incorporates Depth Compensation or Time-Gain Compensation (TGC). This automatically increases the amplification during the time echoes from a particular pulse return, so that the last to arrive are amplified much more than the first. Most of this compensation is built into the machine, but the user can fine-tune it

by means of a bank of slider controls that adjust the amplification at selected depths.

Attenuation artifacts: the intensity of an echo is determined by the product of the ultrasound beam intensity and the structure of the reflecting object. Thus, if the beam is scanning an essentially homogeneous region such as a blood-filled chamber, we would expect the image to appear homogeneous. However, if the beam itself is not homogeneous (typically there is a "hot spot" around the focal zone), then the image in this region will be more intense and generate an artifact that might be interpreted as a mass within the chamber. Such artifacts are usually in the center of the image sector, a few centimeters from the transducer.

The reflection and attenuation characteristics of various media can be used to help in their identification. Referring to Fig. 1.6, with optimized Depth Compensation a soft-tissue structure having slightly different density from its surroundings would be represented as in panel (a). However, within a liquid-filled cystic lesion attenuation is much lower, so the beam beyond it is more intense than in the surrounding tissues, generating a bright "comet tail" as in panel (b). Conversely, an interface with air, such as may be encountered in a cardiac chamber post cardiopulmonary bypass, reflects almost all the incident energy, generating a very bright proximal boundary, and the high attenuation of air strongly attenuates any remaining transmitted beam casting a dark shadow (c).

Reverberation and Multiple Reflection Artifacts

Reverberations: The presence of structures having transmission and attenuation characteristics greatly different from soft tissue is also the cause of reverberation and multiple reflection artifacts, one of the most common sources of misinterpretation of images. Referring to Fig. 1.7, an ultrasound beam crossing a structure normally generates two echoes – one from each interface. However, the echo returning from the further interface has to cross the nearer interface, so part of it is again reflected. This secondary reflection then meets the distant interface a second time, where further reflection occurs, and so on. Under normal circumstances this effect is not seen because soft-tissue

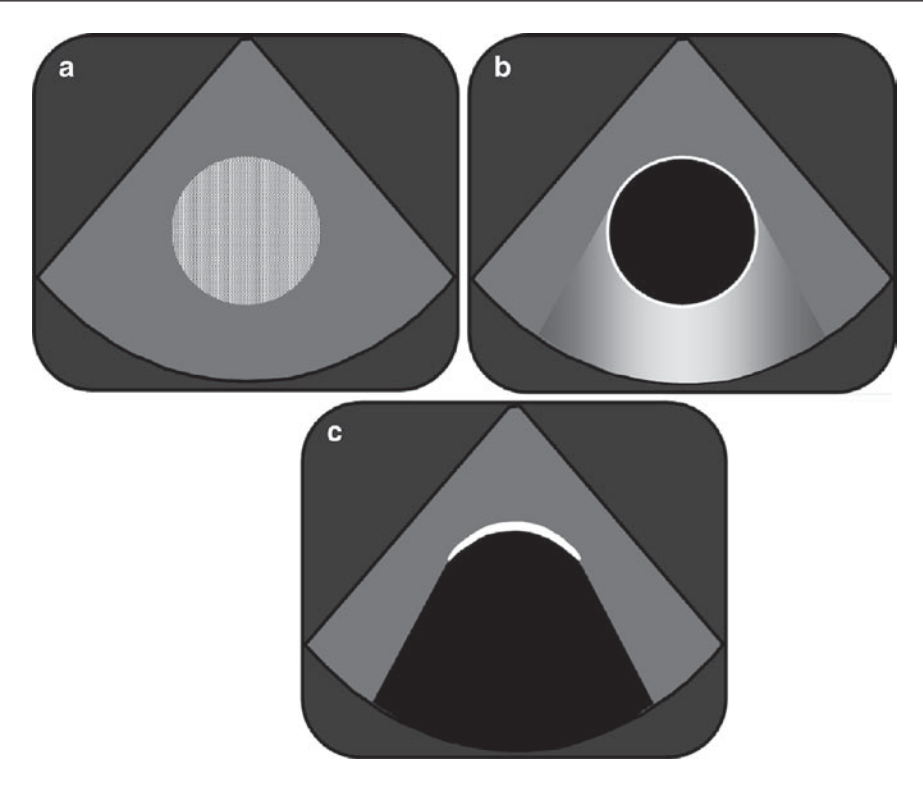


Fig. 1.6 Schematic representation of ultrasound images of (a) a soft-tissue mass, (b) a liquid-filled cyst, and (c) air

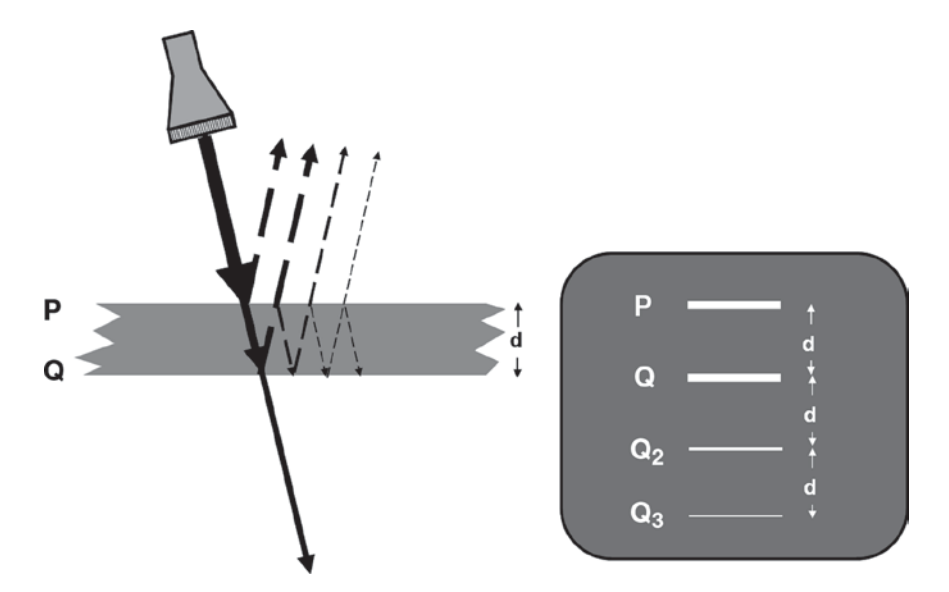


Fig. 1.7 Multiple reflection artifact: If an object generates intense echoes, higher-order reflections are still strong enough to register on the display

reflections are so weak. Thus, if the original echo is 0.1% of the incident wave, the secondary echo has undergone two further reflections and is only $(0.1 \times$

 $0.1 \times 0.1\%$) and too small to register. If, however, the object is a very strong reflector such as a calcified or prosthetic valve with each reflection, say, 10% of the

incident wave then the secondary or higher-order reverberation echoes are strong enough to be detected and are shown as multiple images of the object (Fig. 1.8).

Reflection artifacts: Another consequence of a high-intensity echo is that it can bounce off the transducer face, or a strongly reflecting structure like the pericardium, and back again to the object, creating a secondary "ghost" image (Fig. 1.9). The clue to their recognition is that they are always exactly twice as far away from the transducer as a high-intensity echo, and if the primary structure moves a certain distance, the image generated by multiple reflections moves twice as far.

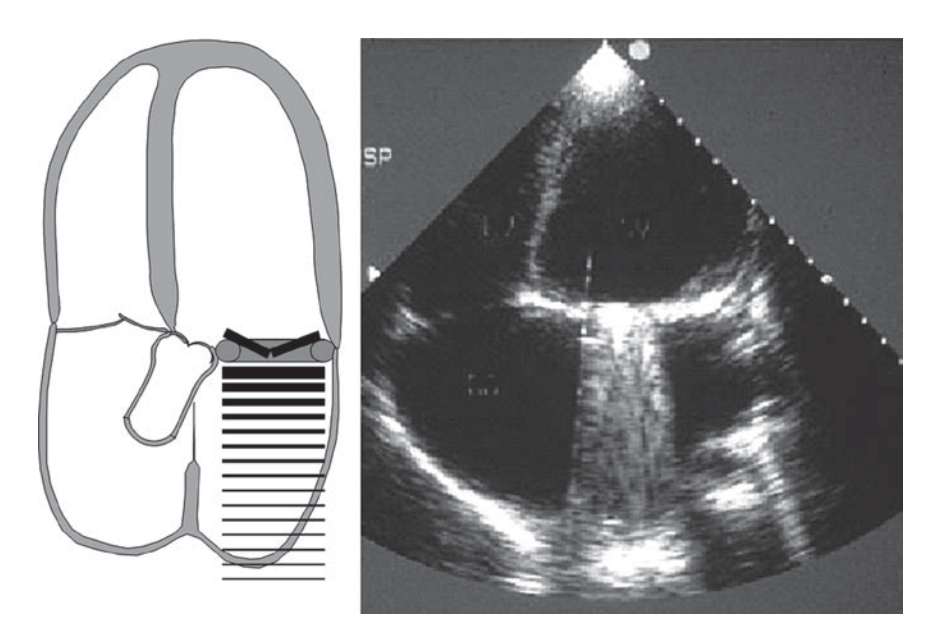


Fig. 1.8 (*Left*) Diagram and (*right*) ultrasound image of a bileaflet prosthetic mitral valve showing multiple reflections from the strongly reflecting hemidiscs. Note how the scan converter has tried to "fill in" the spaces between the echoes

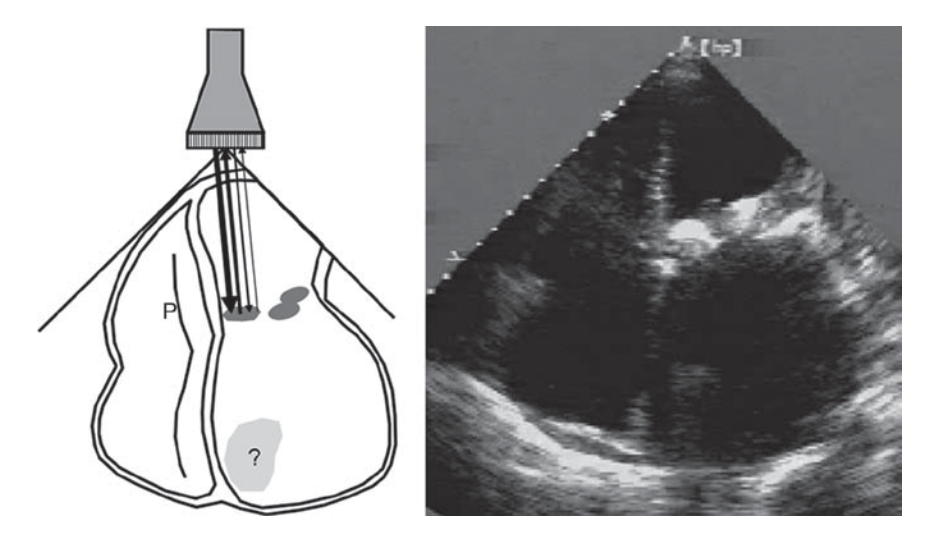


Fig. 1.9 Artifact mimicking a mass in the left atrium resulting from very strong echoes from the calcified mitral valve bouncing off the transducer face

Gray Scale

The intensity of an echo depends on the nature of the tissue interface. As shown earlier, there is a wide range of echo intensities, with a calcified structure generating an echo many thousands of times more intense than a boundary between, say, blood and newly formed thrombus. However, the display system can only represent a fraction of this range (though it may be hard to believe, the difference in light intensity between "black" ink printed on "white" paper is only a factor of 30 or so). Furthermore, the number of gray levels provided in a typical scan converter image memory is only 64. The result is an image with all intense echoes are

shown as "white," all weak echoes as "black," and almost no gray tones. This can to some extent be overcome by compressing the intensity scale to create a softer image, but at the expense of loss of boundary definition (Figs. 1.10 and 1.11).

Resolution of Ultrasound Images

The quality of all images is affected by processing imperfections and random "noise." This is quantified by measuring the resolution, which states how close together two objects can be without their images blurring into one. Resolution in an ultrasound image is

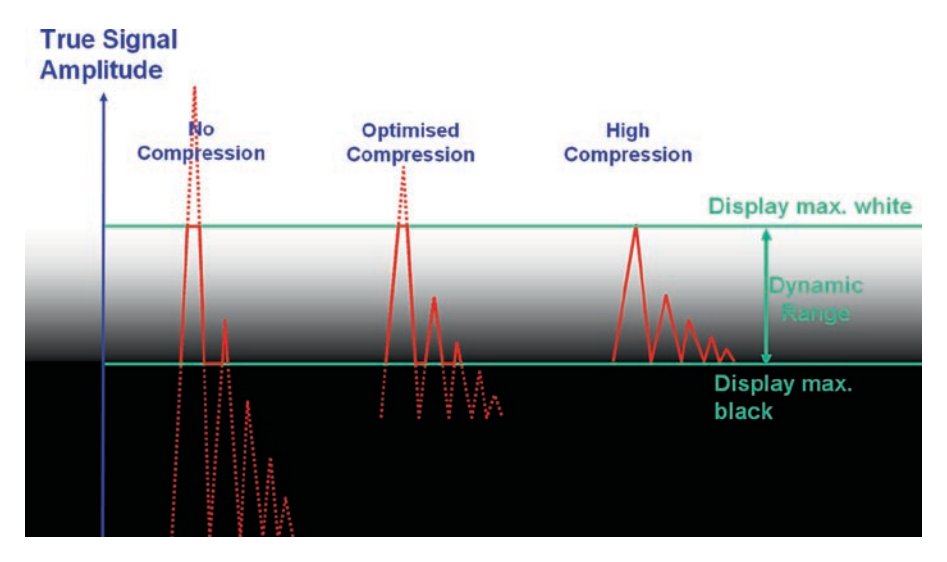


Fig. 1.10 Compression: compressing the echo signal amplitudes helps overcome the very limited dynamic range of the display

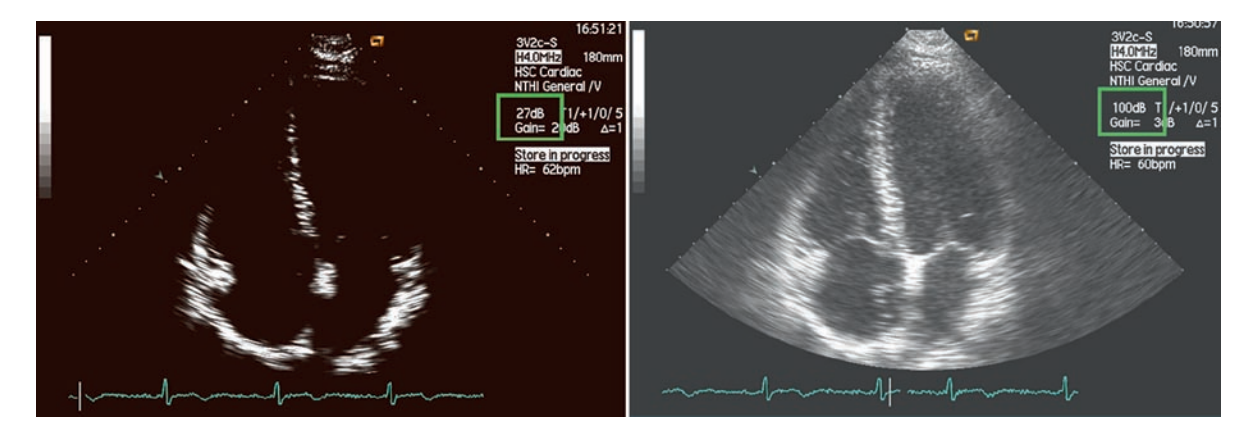


Fig. 1.11 Echo images with (*left*) low gray scale compression (27 dB) giving a harsh "black & white" image and (*right*) high compression (100 dB) resulting in an overly "soft" image

limited by inability to generate infinitely brief pulses and spreading of the beam by diffraction. It is measured along the direction of the beam ("axial" or "range" resolution) and at right angles to the beam direction ("lateral" resolution). The latter is further divided into "azimuthal" resolution, in the plane of the scan, and "elevation" resolution, above and below the scan plane. In a particular imaging system, each of these is different.

Axial resolution: This is determined by the pulse duration. Since each pulse comprises a short burst of waves lasting about 2 ms, with the propagation velocity 1,500 m.s⁻¹, this means that the length of the pulse is about 3 mm. If it encounters an object thinner than this, the front of the wave train comes to the second interface before its tail has crossed the first interface, so the two merge into one echo. Axial resolution can be improved by (a) employing a higher ultrasound frequency, for which the pulse duration is corresponding shorter, and (b) reducing "ringing" by lowering the transmitted power (Mechanical Index).

Lateral resolution is primarily determined by the ultrasound beam width. As shown in Fig. 1.12, if two objects are the same distance from the transducer but sufficiently close together that both are illuminated by

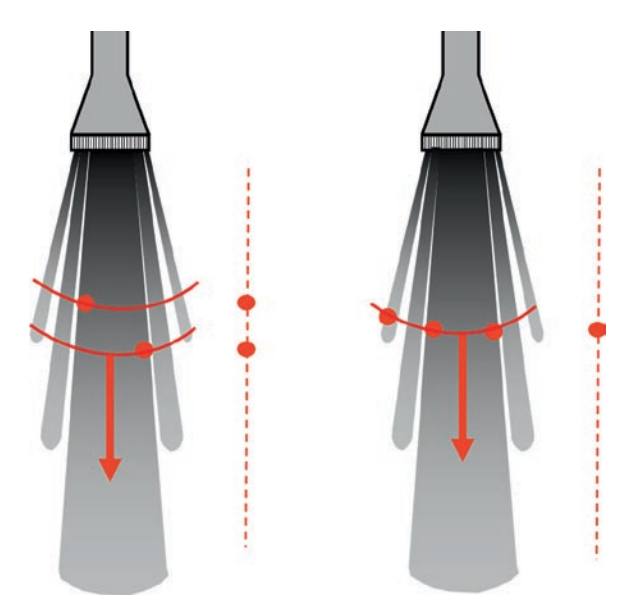


Fig. 1.12 Lateral resolution: (*left*) the ultrasound beam detects only the time taken for echoes to return to the transducer, so only their axial separation is registered. (*Right*) If more than one object is illuminated by the beam at the same range, the echo signals cannot be resolved

the beam (or its side-lobes), then their echoes return simultaneously and cannot be resolved. With the image generated by scanning the beam across the image plane, this means that an object is detected over a range of beam directions, resulting in lateral "smearing" on the display, or multiple representations of a small object such as a pacemaker wire. Lateral resolution is the chief factor limiting the quality of all ultrasound images and is worse than axial resolution, typically by a factor of 10. It can be improved by making the ultrasound beam narrower by focusing it, both in transmit and receive modes. A plastic lens fitted on the face of the transducer focuses the beam both in the azimuthal and the elevation planes, in the same way that a glass lens focuses light, though less effectively. Transducers can be constructed with short-, medium-, or long-focus lenses. In addition, the pulsing sequence in a phased array transducer can be modified to provide additional variable focusing as shown in Fig. 1.13. In most machines, this improves focusing only in the azimuthal plane, but some of the more sophisticated machines have matrix arrays, in which the crystal elements are sliced in two directions, providing the ability for focusing also in the elevation plane. Even so, the beam illuminates unwanted objects, but it is possible also to filter some of these selectively using dynamic receive focusing. As shown diagrammatically in Fig. 1.14, echoes from a particular object do not arrive at all the crystal elements in the transducer simultaneously, but the electrical impulses they generate can be selectively delayed so that those from a particular distance and/or direction reinforce each other, while those from other sources do not. This is analogous to tracking a fastmoving airplane by altering the focus of binoculars as its distance changes.

Minimizing False Diagnoses from Image

- Always use minimum power consistent with obtaining an image
- Beware of "objects" that
 - Are twice as far from the transducer as intense reflectors
 - Lie on an arc centered at the transducer and including an intense reflection
 - Are in the center of the scan sector and a few centimeters from the transducer

If in doubt, see if they are still present when transducer position and image plane are altered

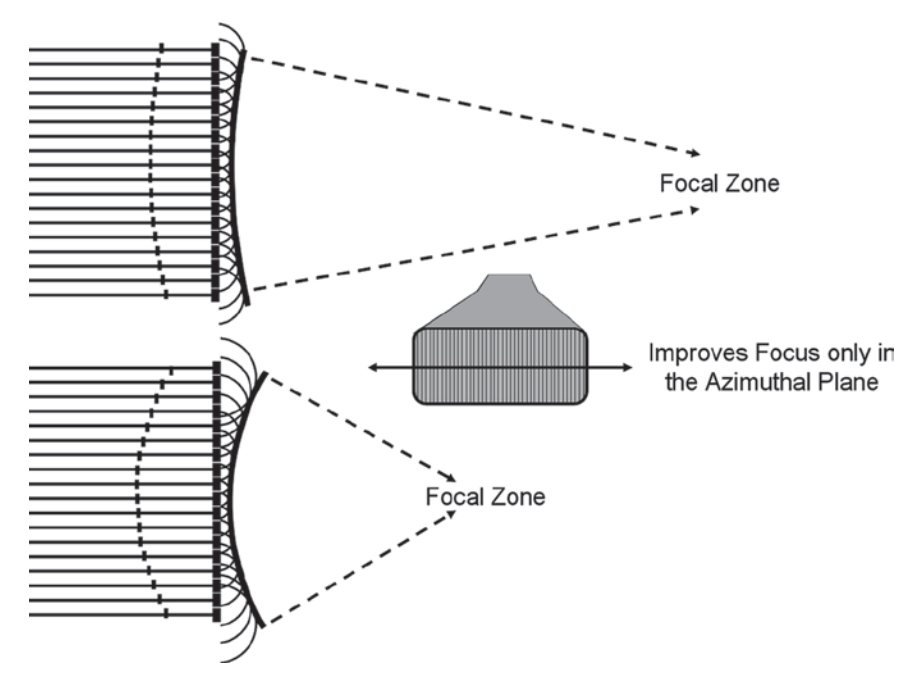


Fig. 1.13 Modification of the electronic pulsing sequence generates a curved wavefront allowing focus in the Azimuthal plane to be adjusted by the operator

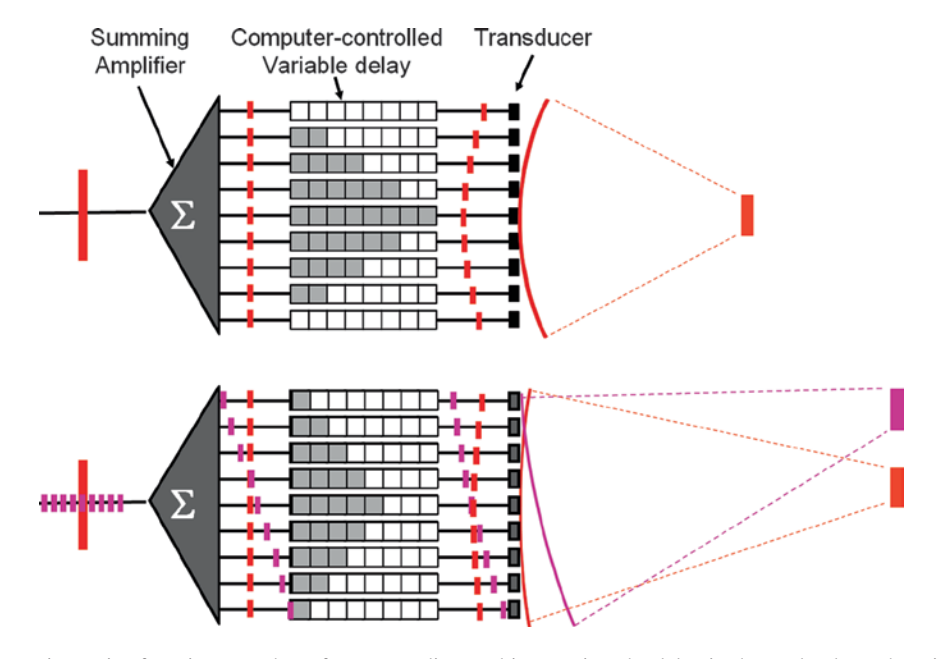


Fig. 1.14 Dynamic receive focusing: as echoes from more distant objects arrive, the delay is changed to keep them in focus, at the same time dispersing off-axis echoes

Parallel Processing

The discussion so far has been based on the formation of images by detecting time echo signals take to return to the transducer and their intensities. Although the transducer contains a number of crystal elements, they act in unison. Image quality is constrained by the scan line density and the beam width. This is not, however,

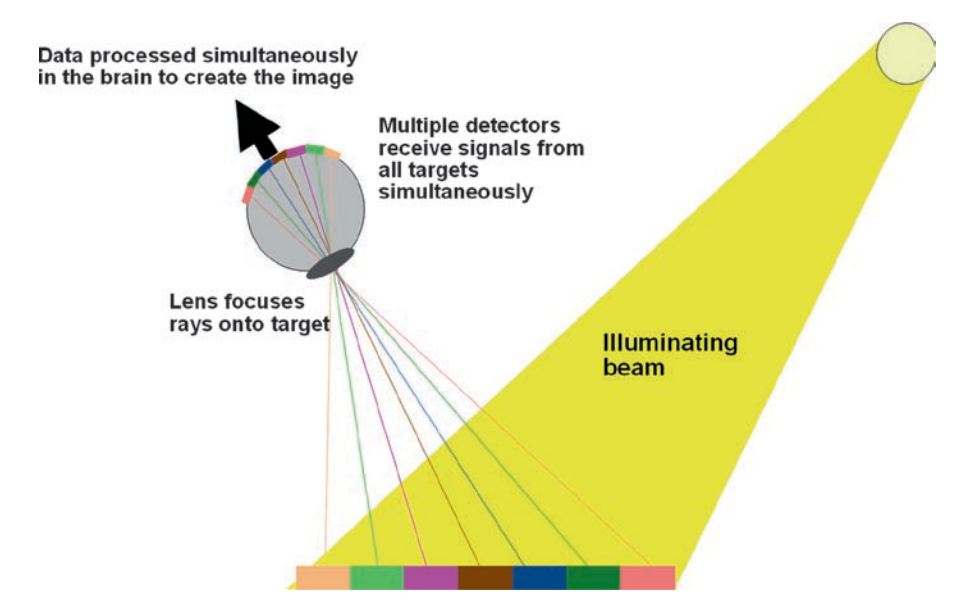


Fig. 1.15 In the eye, a lens focuses reflected light onto an array of detectors, signals from which are processed simultaneously ("parallel processing") by the brain to create the image

the way in which the human eye forms an image (Fig. 1.15). Instead of the eye scanning across the field of view, the scene is flooded with light and image data from it focused onto the millions of individual receptors that comprise the retina. Impulses from these are fed simultaneously to the brain, which processes them to form an image of the complete scene. Why cannot an ultrasound system function similarly? In theory it can, but there are some major practical limitations. The first is that, because of the difference in wavelength, an ultrasound lens would have to be several meters in diameter to be as effective as an optical lens. Secondly, we cannot make transducers with a large number of separate detectors. Thirdly, processing the image data from many detectors simultaneously ("parallel processing") requires more computing power.

However, increased computing power does already allow imaging systems to operate with two parallel processing paths (Fig. 1.16), and this will undoubtedly increase to four or more in time. Even to have two separate detectors provides an enormous benefit because, as with two ears, it provides a directional capability equivalent to a "stereo" music system. A relatively wide ultrasound beam illuminates an area of the heart. An echo from an object in the center of the beam axis arrives simultaneously at the two detector channels, but those from off-axis objects reach one detector channel before the other. The resulting phase

delay allows the computer to assign them to corresponding memory cells. As the beam direction changes, objects previously on the central beam axis are still detected, but their echoes are now out of phase, and can be assigned to the correct memory location, where they add to those from the previous pulse. Several major advantages follow:

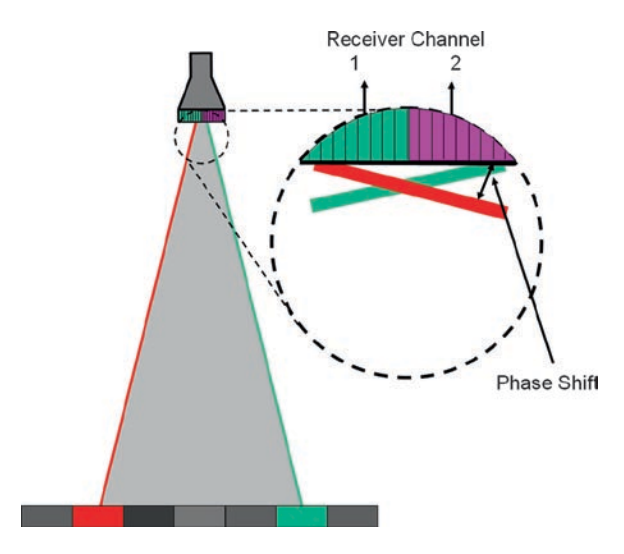


Fig. 1.16 Parallel processing: with two receiver channels, the machine can detect from which part of the illuminated region a particular echo arises

- It is no longer necessary to a very narrow transmitted beam and to have as many transmitted pulses per image, so the frame rate can be increased.
- 2. By detecting both amplitude and phase data, the total amount of information is doubled.
- 3. The image data in each memory cell are built up over several pulses, thus improving sensitivity and reducing noise and allowing higher imaging frequencies to be used with consequent improvement in resolution.

Harmonic Imaging

Fourier's Theorem is a powerful mathematical tool for analyzing waves. It states that any repetitive wave, of whatever shape, can be constructed by adding together a number of regular sine waves of varying frequencies and amplitudes. The basic building block for a particular complex wave is a sine wave having the same frequency and termed the "fundamental." The detail that gives the complex wave its shape is provided by adding to the fundamental further sine waves having frequencies that are exact multiples of that of the fundamental. These are called harmonics (the second harmonic has

twice the frequency of the fundamental, the third harmonic three times, and so on). To form a complex wave perfectly, theory requires an infinite number of harmonics, but their contributions become smaller as the frequency increases, and in practice a fundamental plus ten harmonics provides an adequate representation of the complex wave (Fig. 1.17). The reason why a violin and a trumpet playing the same note sound different is that, though they generate the same fundamental frequency, their harmonic contents are different.

A pure sine wave contains no harmonics, but if its shape is distorted it means that harmonics have been added. This is what happens as an ultrasound pulse travels through the body and it is a consequence of the fact that body tissues, unlike a liquid or solid, are "spongy" and can be compressed relatively easily. As shown in Fig. 1.18, as the positive pressure region of the wave passes through the tissue, it compresses it and the negative part of the wave vice versa. The density of the compressed tissue increases, so the positive pressure part of the wave travels faster and conversely the negative pressure part travels more slowly. The fact that the wave shape changes as it progresses through the body means that it has acquired a harmonic component, which application of Fourier analysis shows is

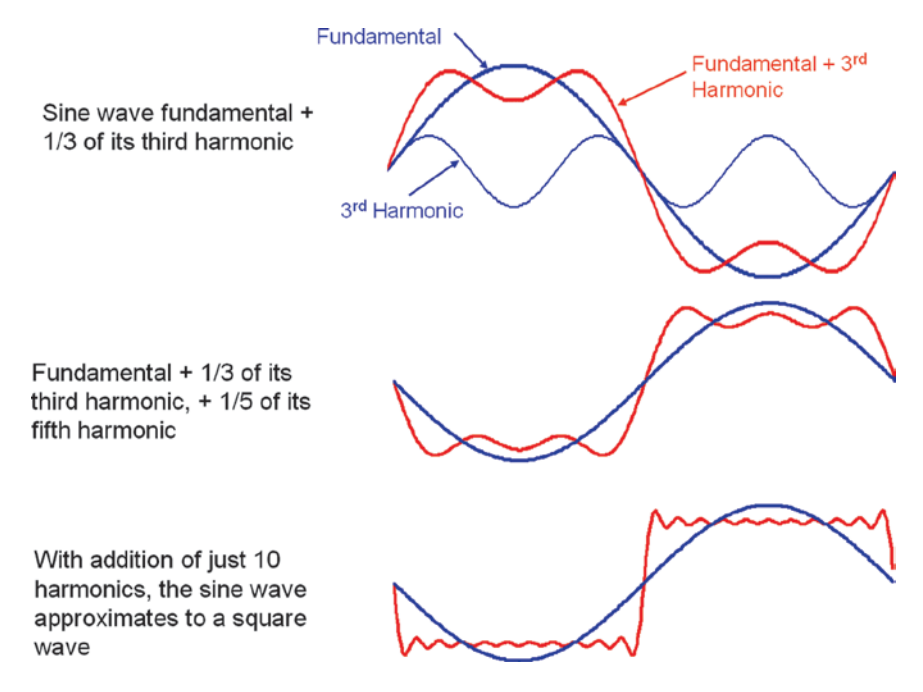


Fig. 1.17 Fourier analysis: the principle by which a complex wave can be created by addition of sine waves or broken down into its sine-wave components

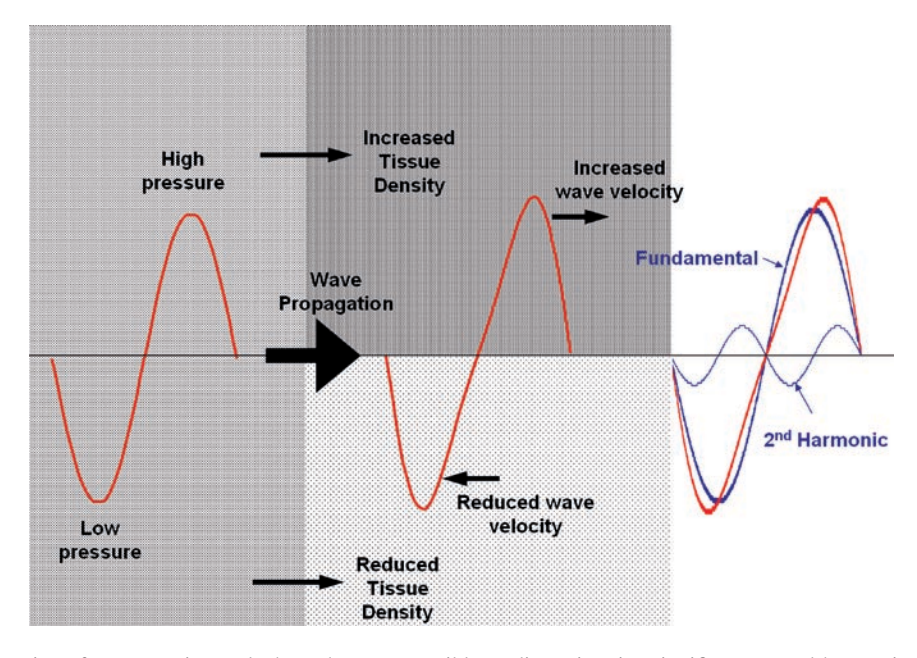


Fig. 1.18 Distortion of a wave as it travels through a compressible medium gives it a significant second-harmonic content

mainly second harmonic, with a smaller proportion of fourth harmonic, and so on.

Thus, when a ultrasound pulse of say, 2 MHz, is transmitted into the body, the echoes that return are not pure 2-MHz sine waves, but include some of its second harmonic (4 MHz), and a little of its fourth harmonic (8 MHz). By selectively filtering out the 2-MHz fundamental, it is possible to form the image from the 4-MHz second harmonic component. This arises mainly from the most intense central part of the beam and, because the wave distortion increases as the transmitted wave travels through the body, there is relatively little harmonic component from proximal structures, and most arises from deeper areas. Harmonic imaging thus provides the following benefits:

- It combines the penetration power of a transmitted low fundamental frequency with the improved image resolution of the harmonic and twice the frequency.
- The harmonic image is preferentially derived from deeper structures and reduces artifacts from proximal objects such as ribs.
- The harmonic image away from the central beam axis is relatively weak and thus not so susceptible to off-axis artifacts.

The improvement in image quality obtained from second harmonic imaging is such that it should be mandatory for all new machine procurement, and machines without it should be regarded as obsolete. There is just one problem associated with harmonic imaging. Because the image is now formed from echoes of a single frequency, some "texture" is lost and structures such as valve leaflets may appear artificially thick. Thus, if the quality of the fundamental frequency image is very good, using the second harmonic mode will offer little benefit and it is best not to use it, but in most patients the improvement in image quality greatly outweighs this minor disadvantage, and in any case manufacturers are likely soon to offer "broad-band" harmonic imaging which will remove the problem.

Transesophageal Imaging

2-D imaging from a phased array transducer positioned in the esophagus has been commercially available since the late 1980s. The transducer (Fig. 1.19) is similar in construction to a gastroscope, but in place of the fiber-optic bundle used for light imaging, a miniature ultrasound transducer is mounted at its tip. This currently has 64 elements (compared with 128 or 256 for transthoracic transducers), but because there is no attenuation from the chest wall, it operates at higher frequencies (up to 7.5 MHz) and produces excellent image quality. Since limited manipulation is possible within the esophagus, the complete transducer array can be rotated by a small electric motor controlled by



Fig. 1.19 Transesophageal transducer

the operator to provide image planes that correspond to the orthogonal axes of the heart despite the fact that these are not naturally aligned with the axis of the esophagus. As mentioned in the section "Is Ultrasound Safe?", special precautions have to be taken to prevent accidental harm to the patient through heating of the transducer. The potential for it to apply 300 volts electrical impulses to the back of the heart also requires it to be checked regularly to ensure integrity of the electrical insulation.

Real-Time 3-D Imaging

If, as well as scanning the ultrasound beam across a linear section of the heart, the entire image plane is scanned up and down, with the echo data fed into a 3-D memory array, it is possible to generate a complete "data set" of the heart's structures rapidly enough to form real-time 3-D images. To achieve this has required overcoming several daunting technological challenges. The first is the construction of the transducer. Instead of cutting a crystal into slices, with wires attached to their edges, the crystal now has to be cut into a matrix of minute squares, each only 2-3 times the width of a human hair, and a wire attached to each one (Fig. 1.20). Even when this is done, the total number of wires is such as to make the connecting cable too unwieldy for clinical use, so the "front-end" beam forming and image processing has to be controlled by electronics built into the transducer, without making it too large or heavy for the operator to hold.

The second problem is to process the enormous amount of data in real time. In the earliest machines real-time imaging has been possible only in parasternal views (where the smaller depth allows higher pulse rates), and even so has involved significant compromises of frame rate and image depth, with a lot of inter-beam smoothing and interpolation. Currently, the image quality is not as good as that of 2-D images, but with ever-increasing computer power it is only a matter of time before this is overcome.

The final problem is that of displaying the data on 2-D video screens. This is done by computer-generated texturing and shadowing to emphasize closer structures and create the impression of a 3-D solid which can be rotated and tilted by a trackball, and from which individual 2-D sections can be extracted (Fig. 1.21). The clinical possibilities for real-time 3-D imaging are enormous, particularly in congenital heart disease, and are only just beginning to be explored.

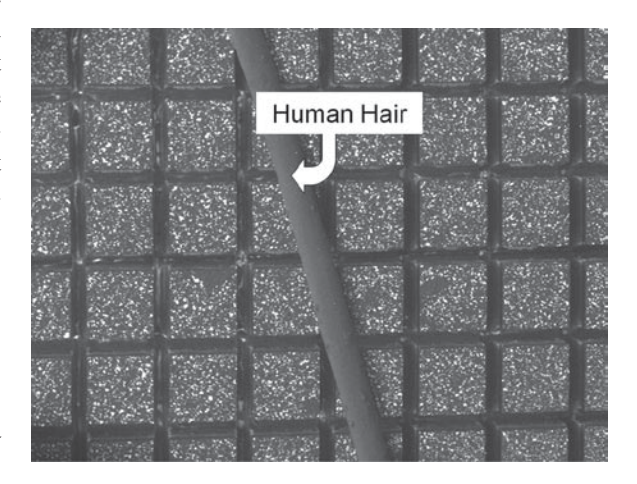


Fig. 1.20 Photomicrograph of the matrix array in a real-time 3-D imaging transducer



Fig. 1.21 Textured 3-D image showing masses attached to both the left and right sides of the interventricular septum

Doppler Echocardiography

Doppler Principles

The specular ultrasound echoes used for imaging the heart are derived from relatively extensive tissue interfaces. When the ultrasound beam encounters much smaller structures, it interacts with them in a completely different way, and instead of being reflected along a defined path, it is scattered equally in all directions just as the circular ripples formed when a small stone is thrown into a pond. The consequence is that most of the incident energy is dissipated, but a small amount returns along the incident path and can be detected, though the resulting signals are much weaker than the specular image echoes. Red blood cells are ideal scatterers; although the echo from a single cell is negligible, signals from millions of them added together can be detected and, if the blood is moving, the frequency of the backscattered echoes is modified by the Doppler effect.

The Doppler effect was first described in 1843 by Christian Doppler, an Austrian mathematician and scientist. He studied the light spectra of double stars and hypothesized that the shifts he observed in the hydrogen spectral lines arose from rotation of the stars about each other. If a star is moving toward the earth the spectral lines are shifted toward blue, and if its

distance is increasing, the shift is toward red. Doppler's theory was confirmed by Buys Ballot in a classical experiment with two trumpeters, one on a moving train and the other on the station. Both played the same note, but observers heard the pitch of the note from the passing train change as it first approached then receded. As the wave source moves toward the observer, the waves are compressed, decreasing the wavelength and increasing the pitch, and as the source moves away from the observer, the apparent wavelength increases and pitch lowers.

Thus, if an ultrasound beam encounters a stream of moving blood, returning backscattered echoes have a slightly different frequency from that of the transmitted beam, the difference being known as the Doppler shift or Doppler frequency. The Doppler equation (Fig. 1.22) shows how this can be used to calculate the blood flow velocity. For a velocity of 1 m.s⁻¹ and ultrasound frequency 2.5 MHz the Doppler shift is about 3.3 kHz, only 0.1%, but readily detected and directly proportional to the blood velocity. Note, however, that, application of the Doppler equation requires that that the angle between the beam axis and blood flow direction either must be known or must be so small that its cosine is effectively unity. Also, the Doppler shift for a given blood velocity is related to the ultrasound frequency, so is twice as large for the same blood velocity at 5 MHz as for 2.5 MHz.

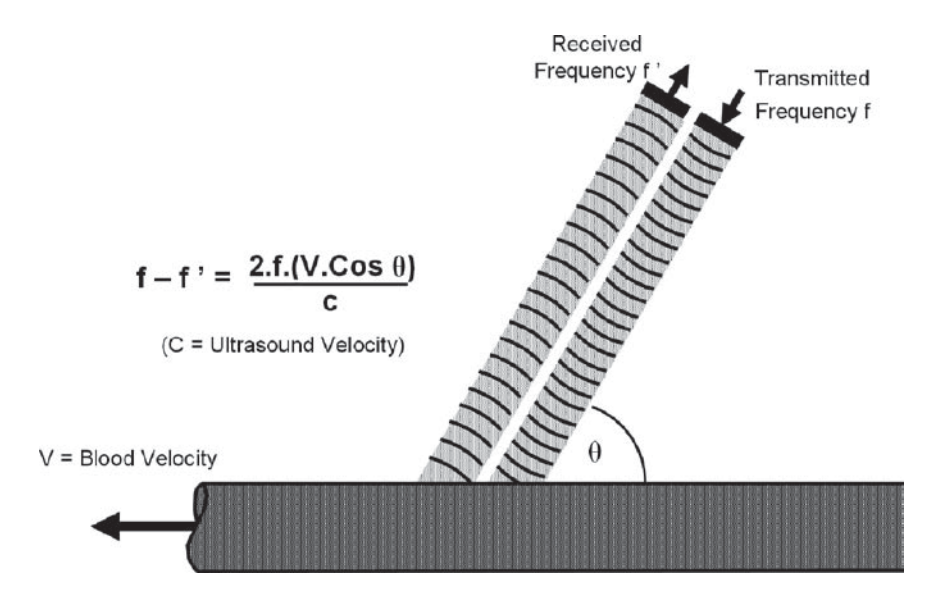


Fig. 1.22 The Doppler equation, relating flow velocity to the ultrasound "Doppler Shift"

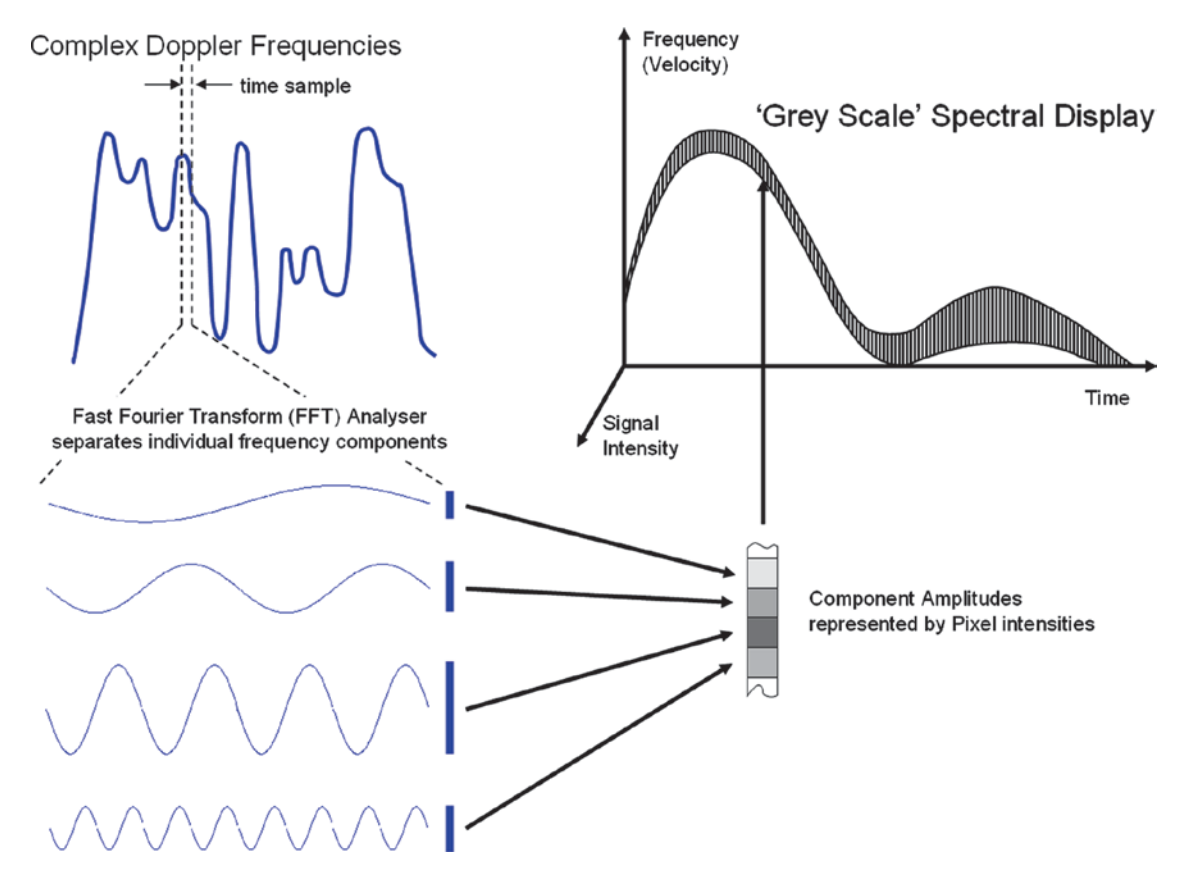


Fig. 1.23 Breaking down a complex waveform into its sine-wave components to generate a spectral Doppler display

In practice, blood in an artery does not all flow at the same velocity, due to friction at the walls. Furthermore, with pulsatile flow the velocity is constantly changing, resulting in complex flow patterns. The interrogating ultrasound beam does not therefore return just one Doppler shift, but a spectrum of frequencies, like the orchestra tuning up before a performance. The complex mix of Doppler shifts is analyzed and the resulting velocity data used to generate a Spectral Doppler Display (Fig. 1.23). This shows the range of velocities detected at each point in the cardiac cycle, with flow toward the transducer shown above the baseline and flow away from the transducer below it. The density of the image shows the amplitude of the signal at each Doppler shift, which depends on the number of scatterers, and thus the proportion of blood flow at that velocity. A line tracing the outer edge of the spectrum shows the peak velocity and a line through the center of the band approximates to the mean velocity (Fig. 1.24).

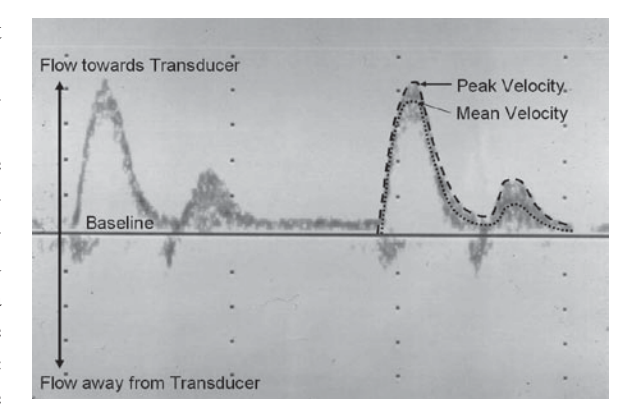


Fig. 1.24 Spectral Doppler display of flow in a carotid artery

Continuous-Wave Spectral Doppler

Instead of the brief pulses used for imaging, Continuous Wave (CW) Doppler requires transmission of a

continuous train of sinusoidal ultrasound waves and simultaneous reception of the returning backscattered echoes. This is achieved either by using a special dedicated transducer (commonly referred to as a "pencil probe") containing two separate crystals, or by assigning the crystal elements in the imaging transducer to two groups, one for transmission and the other to detect the echoes. CW Doppler provides quantitative data on blood velocities of any magnitude, enabling flow volumes and pressure gradients to be calculated.

Volumetric Flow

For steady-state flow, the volume of liquid flowing through a pipe in a given time is the product of the cross-sectional area of the pipe, the mean velocity, and the time interval (A × V × T). If flow is pulsatile, as in Fig. 1.25, the product of (velocity × time) is replaced by the velocity-time integral $\int_0^T V.dT$. This is represented by the shaded area under the spectral display and has the dimension of distance (velocity × time = distance). It is called the "Stroke Distance" and in physiological terms it is the measure of the distance that an element of the fluid travels during one pumping cycle.

The Continuity Equation and Flow Through a Restricting Orifice

Referring to Fig. 1.26, if a fluid, which is not compressible, flows along a rigid-walled pipe, the amount entering one end of the pipe must be the same as that leaving the other end. If the diameter of the pipe changes, this still holds true, so a reduction in cross-sectional area is compensated for by an increase in mean velocity. This principle, known as the Continuity Equation, can be expressed as $A_1 \times V_1 = A_2 \times V_2$. Provided three of the terms in the equation are known, the fourth can be derived. This is used, for example, to determine the valve orifice area in aortic stenosis. The orifice is too small and irregular to be measured directly, but if the area of the outflow tract upstream is measured, together with the up-stream and trans-valvar velocities, then the valve area can be calculated.

Liquid only flows along a pipe if there is a pressure difference between its ends. For a fixed pipe diameter and steady-state flow, only a small pressure gradient is

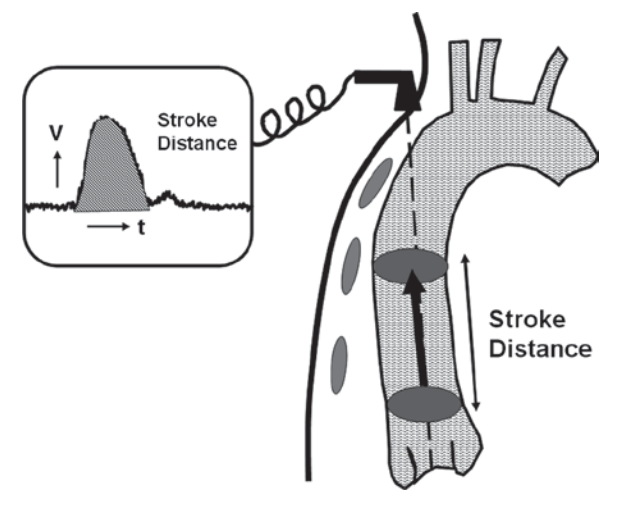


Fig. 1.25 The "Stroke Distance" is calculated by measuring the systolic area of the spectral flow display and corresponds to the distance blood travels along a vessel during one cardiac cycle



Same volume per second flows in each section, therefore: $A_1 \times V_1 = A_2 \times V_2$

Fig. 1.26 The Continuity equation

required to overcome frictional losses, but when the pipe becomes narrower, its velocity increases and the additional kinetic (motion) energy it thus acquires requires a higher pressure gradient.

Neglecting the frictional and turbulence losses, the relationship between pressure and velocity is:

$$P_1 - P_2 = 1 / 2\rho(V_2^2 - V_1^2)$$

where V_1 , P_1 and V_2 , P_2 are the up-stream and down-stream velocities and pressures, and r is the density of the liquid. This is simply a statement of the Newtonian principle of Conservation of Energy applied to fluids and was first derived by Daniel Bernoulli in the mideighteenth century.

Figure 1.27 shows the application of Bernoulli's equation to the pressure-velocity relationships in mitral valve stenosis. In this example and most clinical cases of obstructed blood flow (valve stenoses, aortic coarctation, restrictive VSD, etc.), the upstream velocity is small compared to the downstream velocity, and the